# Optimal Low-Thrust Escape Trajectories Using Gravity Assist

Lorenzo Casalino,* Guido Colasurdo,† and Dario Pastrone‡
*Politecnico di Torino, 10129 Turin, Italy*

Electric propulsion provides a spacecraft with continuous steering capabilities, which can be used to approach a planet with hyperbolic excess velocity that enhances the gravity assist. Low-thrust trajectories to escape from the solar system are considered in the present paper, which searches for the strategy that maximizes the spacecraft energy for assigned payload and engine operating time. The optimal conditions to escape using electric propulsion and gravity assist are presented for the cases of free-height and minimum-height flybys. Optimal trajectories that exploit Jupiter or Venus flybys have been computed for constant exhaust power with either constant or variable specific impulse; the procedure is also able to determine the optimal power level and to suggest when it is convenient to switch the engine on and off. The benefit that system performance can receive by increasing the number of controls, i.e., by adding the possibility of coast arcs and engine throttling to the thrust direction control, is also noted.

## Introduction

THE first mission of the New Millenium Program, Deep Space 1, has recently begun; the spacecraft uses an ion thruster for primary propulsion. Other more ambitious missions aimed at deep-space exploration will probably use electric propulsion in the near future. The thrust acceleration will be comparable to the solar gravitational acceleration as the missions cannot last too many years (i.e., revolutions around the sun). In these cases the simplest steering strategies, which use either thrust parallel to the spacecraft velocity or perpendicular to the sun-spacecraft direction, produce rather poor system performance in comparison to the steering strategies that are suggested by direct or indirect optimization procedures. The authors prefer and currently use the indirect approach; this optimization technique has already been applied to this kind of trajectory[1−3] and guarantees excellent numerical accuracy. The convergence of the numerical procedure is not difficult, as related problems usually arise for very low thrust levels that are typical of geocentric trajectories.

The opportunities of exploiting a gravity assist en route to deep space must be considered.[4] Electric propulsion adds steering capabilities, which should be used to approach the planet with the best direction for the gravity assist; this possibility is precluded in the simplest steering strategies and is not usually considered in the applications of indirect optimization procedures. This paper presents the equations and conditions that must be satisfied by a trajectory that makes optimal use of both propellant and gravity assist. The patched-conic approach is adopted, but the spacecraft trajectory is analyzed only in the heliocentric reference frame, as the elapsed time inside the planets' spheres of influence is neglected and flybys are considered as discontinuities between powered heliocentric arcs.[5]

The use of a nuclear power source is mandatory during deep-space missions; a constant-power trajectory is related to this kind of mission. The mass of the power source, which reduces the payload, is roughly proportional to the exhaust power. The optimal value of the power level is determined, with the engine operation, using constant thrust magnitude (and specific impulse), analyzed first. A constant-power engine that can be throttled (i.e., that uses the best combination of thrust magnitude and specific impulse at any instant)

is then considered. As the thruster life is generally time-limited,[6] the possibility of a temporary engine switch-off is taken into account; it may be useful to save propulsive resources and exploit them under better circumstances, for instance, after the flyby, when the gravity assist has increased the spacecraft velocity.

A rather simple mission is considered so as to avoid the peculiar characteristics of a too complex mission that could affect the discussion of the main topics of the present analysis. These topics concern the benefit arising from the possibility of steering the spacecraft up to the time of the flyby and judiciously throttling the engine. The same benefits pertain to both nuclear and solar propulsion; for the sake of simplicity a nuclear (i.e., constant-power) generator is assumed. A spacecraft with an assigned payload ratio leaves the Earth's sphere of influence with a fixed hyperbolic excess velocity; the maximum heliocentric specific energy after an assigned engine operating time is determined. The planets' orbits around the sun are assumed to be circular and coplanar. The problem becomes independent of the departure time, and the optimal trajectory is accordingly computed. The initial phase angle between the relevant planets, i.e., the departure time, is found a posteriori. However, this approximation could be removed, and only a minor complexity would be added to the boundary conditions.[5] The simplified approach is preferred here, as the comparison of different control modes is unaffected by the time length of the trajectory that moves the spacecraft from the Earth to the planet that provides the gravity assist.

The optimal conditions for more complex missions using high-thrust propulsion have recently been presented.[5,7] The discussion of the optimal conditions, which are substantially independent of the propulsion system, is here only summarized to pay greater attention to the analysis of the optimal controls that are peculiar of electric propulsion. The preliminary results of a work in progress concerning missions to near-Earth asteroids show that the same technique can successfully deal with time-constrained nonplanar problems using either nuclear or solar electric propulsion.

## Statement of the Problem

The present analysis considers the heliocentric phase of an interplanetary mission; for the sake of simplicity, the planets' orbits are considered to be circular and coplanar. All variables are made nondimensional by assuming the radius of Earth's orbit $r_{ref} = 1$ AU $= 149.6 \times 10^6$ km, the corresponding circular velocity $v_{ref} = 29.785$ km/s, and the spacecraft initial mass as reference values. The objective of the optimization procedure is to maximize the final value of the spacecraft specific energy, when the engine operating time $\tau$ and payload $m_u$ are assigned. The spacecraft leaves the Earth's sphere of influence with an assigned magnitude of the hyperbolic excess velocity $v_{\infty 0}$; its direction is instead subject to optimization.

*Researcher, Dipartimento di Energetica, Corso Duca degli Abruzzi, 24. Member AIAA.

†Professor, Dipartimento di Energetica, Corso Duca degli Abruzzi, 24. Senior Member AIAA.

‡Associate Professor, Dipartimento di Energetica, Corso Duca degli Abruzzi, 24. Member AIAA.

The equations of motion of the spacecraft under the influence of its thrust $\boldsymbol{T}$ and the sun's gravitational acceleration $\boldsymbol{g}(\boldsymbol{r})$ are

$$\dot{\boldsymbol{r}} = \boldsymbol{v}, \qquad \dot{\boldsymbol{v}} = \boldsymbol{g} + \boldsymbol{T}/m, \qquad \dot{m} = -T/c \qquad (1)$$

where the propellant mass-flow rate is expressed by the ratio of the thrust magnitude to the exhaust velocity $c$.

To apply the theory of optimal control, the Hamiltonian function

$$H = \boldsymbol{\lambda}_r^T \boldsymbol{v} + \boldsymbol{\lambda}_v^T (\boldsymbol{g} + \boldsymbol{T}/m) - \lambda_m T/c \qquad (2)$$

is defined. The problem is autonomous, and $H$ is piecewise constant (it may experience jumps where state variables or controls are discontinuous). Different control modes are considered in the paper; the thrust direction is always used to improve system performance; and the exhaust power $P = Tc/2$ and the exhaust velocity $c$ constitute two additional controls when the thruster can be switched off or continuously throttled, respectively. The Euler–Lagrange conditions provide adjoint equations for the problem

$$\dot{\boldsymbol{\lambda}}_r^T = -\boldsymbol{\lambda}_v^T G, \qquad \dot{\boldsymbol{\lambda}}_v^T = -\boldsymbol{\lambda}_r^T, \qquad \dot{\lambda}_m = \boldsymbol{\lambda}_v^T \boldsymbol{T}/m^2 \qquad (3)$$

where $G(\boldsymbol{r})$ is the gravity-gradient matrix $\partial \boldsymbol{g}/\partial \boldsymbol{r}$.

## Boundary Conditions

The trajectory is divided into arcs by the points where state or control variables experience jumps; the boundary conditions at the arc junctions are obtained by means of the following expressions[8,9] (subscripts − and + distinguish the values just before and after the junction):

$$\left( H_{j_-} + \frac{\partial \varphi}{\partial t_{j_-}} + \boldsymbol{\mu}^T \frac{\partial \boldsymbol{\chi}}{\partial t_{j_-}} \right) \delta t_{j_-} = 0 \qquad (4)$$

$$\left( H_{j_+} - \frac{\partial \varphi}{\partial t_{j_+}} - \boldsymbol{\mu}^T \frac{\partial \boldsymbol{\chi}}{\partial t_{j_+}} \right) \delta t_{j_+} = 0 \qquad (5)$$

$$\left( \boldsymbol{\lambda}_{j_-}^T - \frac{\partial \varphi}{\partial \boldsymbol{x}_{j_-}} - \boldsymbol{\mu}^T \frac{\partial \boldsymbol{\chi}}{\partial \boldsymbol{x}_{j_-}} \right) \delta \boldsymbol{x}_{j_-} = 0 \qquad (6)$$

$$\left( \boldsymbol{\lambda}_{j_+}^T + \frac{\partial \varphi}{\partial \boldsymbol{x}_{j_+}} + \boldsymbol{\mu}^T \frac{\partial \boldsymbol{\chi}}{\partial \boldsymbol{x}_{j_+}} \right) \delta \boldsymbol{x}_{j_+} = 0 \qquad (7)$$

where $\boldsymbol{\chi}$ is the vector of the constraining equations and $\varphi$ the function that must be maximized. In this case $\varphi = CE_f = C(v_f^2/2 - 1/r_f)$ is an arbitrary multiple of the spacecraft energy at the final point (subscript $f$). The necessary optimum conditions, which are obtained by applying Eqs. (4–7), have been presented by the authors in previous papers[3,5,7] and are summarized here.

At the initial point (subscript 0) the position vector $\boldsymbol{r}_0 = \boldsymbol{r}_\oplus$, the magnitude of the hyperbolic excess velocity $(\boldsymbol{v}_0 - \boldsymbol{v}_\oplus)^2 = v_{\infty 0}^2$, and the nondimensional initial mass $m_0 = 1$ are assigned. Necessary optimum conditions state that $\boldsymbol{\lambda}_{v0}$ must be parallel to the hyperbolic excess velocity; $\boldsymbol{\lambda}_{r0}$ and $\lambda_{m0}$ are free. The unspecified value of the constant $C$ is used to make the tangential component of $\boldsymbol{\lambda}_{v0}$ unity.

The radius is assigned, and the magnitude of the hyperbolic excess velocity is the same just before and after a flyby (subscript $i$); for instance, in the case of the Jupiter ($\mathbf{2\!\!\!+}$) flyby, $r_{i+} = r_{i-} = r_{\mathbf{2\!\!\!+}}$ and $(\boldsymbol{v}_{i+} - \boldsymbol{v}_{\mathbf{2\!\!\!+}})^2 = (\boldsymbol{v}_{i-} - \boldsymbol{v}_{\mathbf{2\!\!\!+}})^2$. If a minimum-height flyby is performed, a condition on the velocity turn is added

$$\boldsymbol{v}_{\infty+}^T \boldsymbol{v}_{\infty-} = -\cos 2\phi\, v_{\infty-}^2 \qquad (8)$$

where

$$\cos \phi = \frac{v_p^2}{v_{\infty-}^2 + v_p^2} \qquad (9)$$

and $\boldsymbol{v}_{\infty\pm} = \boldsymbol{v}_{i\pm} - \boldsymbol{v}_{\mathbf{2\!\!\!+}}$ and $v_p$ is the circular velocity at the minimum allowable distance from the planet. Equations (6) and (7) state that $\boldsymbol{\lambda}_{vi}$ must be parallel to the hyperbolic excess velocity just before

and after the free-height flyby; its magnitude is continuous. On the contrary, if a minimum-height flyby is performed, the component $\lambda_{vi}^\perp$, normal to the hyperbolic excess velocity, is constant, whereas the parallel component $\lambda_{vi}^\parallel$ is discontinuous according to

$$\lambda_{vi+}^\parallel = \lambda_{vi-}^\parallel + 2A\lambda_{vi-}^\perp \qquad (10)$$

where

$$A = \frac{\mathrm{d}\phi}{\mathrm{d}\boldsymbol{v}_{\infty-}} \boldsymbol{v}_{\infty-} \qquad (11)$$

In both cases $\boldsymbol{\lambda}_{ri}$ presents a free discontinuity, whereas $\lambda_{mi}$ is continuous. Equations (4) and (5) are used to obtain transversality conditions that implicitly determine the arc time lengths; they state the Hamiltonian's continuity across the flyby maneuver.

At the final point $\boldsymbol{\lambda}_{vf}$ must be parallel to the velocity, $\boldsymbol{\lambda}_{rf}$ to the radius, and $\boldsymbol{\lambda}_{rf}^T \boldsymbol{v}_f + \boldsymbol{\lambda}_{vf}^T \boldsymbol{g} = 0$. The final values of $\lambda_{mf}$ and $H_f$ depend on the control mode that has been considered, as is shown in the next section.

Polar coordinates $(r, \vartheta)$ with radial and tangential velocity components are used in coplanar problems. Throughout the present analysis the planets move on circular orbits, and the most favorable phase angle between them is always assumed; one is allowed to pose $t_0 = \vartheta_0 = 0$ and to let the planet's angular position at the flyby be unconstrained. The adjoint variable $\lambda_\vartheta$ is zero during the whole trajectory.

## Optimal Controls

Pontryagin's Maximum Principle states that the controls must maximize the Hamiltonian; thus, the optimal thrust direction must be parallel to the velocity adjoint vector $\boldsymbol{\lambda}_v$, which is usually called the *primer vector*.[10] By remembering that $T = 2P/c$, Eq. (2) is rewritten as

$$H = \boldsymbol{\lambda}_r^T \boldsymbol{v} + \boldsymbol{\lambda}_v^T \boldsymbol{g} + (2P/c)(\lambda_v/m - \lambda_m/c) \qquad (12)$$

The additional controls $P$ and $c$ are made evident by Eq. (12); it will be shown that optimal performance is produced by a bang-bang control of the exhaust power, i.e., the thruster either operates at its maximum power level $P^*$ or is switched off. For the sake of simplicity, the engine efficiency, that is, the efficiency of the conversion of the electrical power into beam power, is considered to be constant, and the mass of the power source is considered to be proportional to $P^*$ via the power source specific mass $\beta$. The payload is then expressed as

$$m_u = m_f - \beta P^* = 1 - m_p - \beta P^* \qquad (13)$$

where $m_f$ is the final mass and $m_p$ the propellant mass. The propellant tank mass is neglected; however, it could easily be taken into account.[4]

### Constant Exhaust Velocity

When the thruster can operate only with constant exhaust velocity, Eq. (12) is usually written in the form

$$H = \boldsymbol{\lambda}_r^T \boldsymbol{v} + \boldsymbol{\lambda}_v^T \boldsymbol{g} + T S_T \qquad (14)$$

where

$$S_T = \lambda_v/m - \lambda_m/c \qquad (15)$$

To maximize the Hamiltonian according to Pontryagin's Maximum Principle, thrust and exhaust power must assume their maximum values when the switch function $S_T$ is positive, whereas they must be set to zero when $S_T < 0$.

If the maximum exhaust power is assigned, the propellant mass is

$$m_p = (T/c)\tau = (2P^*/c^2)\tau \qquad (16)$$

and the required payload, via Eq. (13), prescribes the exhaust velocity

$$c = \sqrt{\frac{2P^*\tau}{1 - m_u - \beta P^*}} \qquad (17)$$

The constraint on the engine operating time is enforced by means of the same Eq. (13), which is rewritten as

$$m_f = m_u + \beta P^* \qquad (18)$$

In this case, the final mass is assigned, and $\lambda_{mf}$ is free. No constraint is explicitly posed on the final time, and one obtains $H_f = 0$; this condition is equivalent to $S_{Tf} = 0$ because of the other boundary conditions at the end point.

The final time is actually free, and the optimal solution would imply an infinite number of negligibly short thrust arcs. Numerical examples search for the best solution corresponding to an assigned switching structure, that is, an assigned sequence of thrust and coast arcs. In particular, two cases are considered: the continuous use of thrust and the insertion of a single coast arc between two full-power arcs. In the latter case the application of Eqs. (4) and (5) states the necessary continuity of the Hamiltonian at the arc junctions, which is assured by enforcing $S_T = 0$ there. It is necessary to remark that the switching structure must also consider the flyby position; in the examples the last or unique powered phase is actually split into two powered arcs by the flyby.

The optimization procedure can also furnish the optimal value of the beam power, i.e., the mass of the power source: it is sufficient to consider $P^*$ as an additional state variable that is constant over the whole trajectory. An adjoint variable is then introduced whose time derivative is null during the coast arc ($P = 0$); during the propelled arcs ($P = P^*$),

$$\dot{\lambda}_P = -\frac{\partial H}{\partial P^*} = -\frac{\lambda_v}{m}\frac{c(1 - m_u - 2\beta P^*)}{2P^*\tau} - \lambda_m\frac{\beta}{\tau} \qquad (19)$$

is obtained by taking Eq. (17) into account. As the initial value for $P^*$ is unconstrained, $\lambda_{P0} = 0$. Equation (18) now contains two state variables and produces the necessary condition for optimality:

$$\lambda_{Pf} + \beta\lambda_{mf} = 0 \qquad (20)$$

### Variable Exhaust Velocity

If the thruster can be continuously throttled, the exhaust velocity becomes an additional control variable; its optimal value is obtained by nullifying the Hamiltonian partial derivative with respect to $c$ itself. One obtains[2]

$$c = 2m\lambda_m/\lambda_v \qquad (21)$$

which maximizes the Hamiltonian as the second partial derivative of $H$ with respect to $c$ is easily found to be unconditionally negative. Equation (12) can be written in the form

$$H = \boldsymbol{\lambda}_r^T\boldsymbol{v} + \boldsymbol{\lambda}_v^T\boldsymbol{g} + PS_P \qquad (22)$$

where

$$S_P = \frac{\lambda_v^2}{2m^2\lambda_m} \qquad (23)$$

The switch function $S_P$ is always positive, but the Appendix shows that the presence of a coast arc may improve the solution when the time constraint concerns the engine operating time instead of the overall time length of the trajectory.

The optimization procedure does not strictly conform to the Appendix. The switching structure is preliminarily assigned also in this case. Equation (18) is now not sufficient to constrain the engine operating time, and a time constraint is explicitly imposed ($t_f = \tau$, if the thruster cannot be turned off; $t_f - t_{2+} + t_{1-} = \tau$, if a coast arc is inserted between points 1 and 2). Both $\lambda_{mf}$ and $H_f$ are free (and $S_{Pf} \neq 0$). The application of Eqs. (4) and (5) states that the Hamiltonian is discontinuous, and $S_P = S_{Pf}$ at the arc junctions, where the engine is switched off or on.

The optimal value of the maximum exhaust power $P^*$ could be found by the procedure also in this case; the $\lambda_P$ time derivative during the propelled arcs is now

$$\dot{\lambda}_P = -\frac{\partial H}{\partial P^*} = -S_P \qquad (24)$$

The boundary conditions are again $\lambda_{P0} = 0$, together with Eqs. (18) and (20). However, the optimal power depends only on $m_u$ and $\beta$: in fact, it can easily be shown that $P^*\lambda_P + m\lambda_m$ and $m^2\lambda_m$ are first integrals of the motion, i.e., are constant during the whole trajectory. Therefore, $P^*\lambda_{Pf} + m_f\lambda_{mf} = \lambda_{m0}$ and $m_f^2\lambda_{mf} = \lambda_{m0}$. By considering Eqs. (18) and (20), one obtains $m_f^2 = m_u$, and, consequently, the optimal power $P^* = [\sqrt{(m_u)} - m_u]/\beta$. This value is known a priori, and Eq. (24) is actually not integrated.

One should also note that the thrust acceleration $\boldsymbol{T}/m = P^*\boldsymbol{\lambda}_v/(m^2\lambda_m)$ is proportional to the primer ($m^2\lambda_m$ is constant), as has been found by Prussing[1] and Kechichian.[2]

## Numerical Examples

The boundary-value problem that arises from the application of the theory of optimal control is solved by means of a shooting procedure[11] that exploits the numerical integration of the sensitivity equations. The solver efficiency is improved by a particular treatment of the interior boundary points that allows the simultaneous optimization of the whole trajectory instead of matching separately optimized arcs. The solver is very accurate; the optimal solution is achieved with an eight-digit precision in about 10 iterations and 20 s using a high performance PC if the initial guess is close enough to allow the convergence of the procedure. The convergence is in fact easily obtained when the solution of a similar problem is known, that is, once the solution for any mission of a new class has been found.

Two numerical examples (i.e., two classes of mission) are presented. The first one employs a Jupiter flyby to escape from the solar system; the technological level necessary for such a mission is beyond the present capabilities. The engine operating time is $\tau = 10\pi$ (5 years); other data are $m_u = 0.5$, $v_{\infty 0} = 0.1$ (2.98 km/s), and $\beta = 10$ (about 57 kg/kW). Different control modes are compared; the results are summarized in Table 1. The second example deals with a Venus flyby and assumes a lower technological level ($\tau = 4\pi$, $\beta = 25$); only the best solution is presented.

In the first example a constant specific impulse and a continuous use of the thruster is initially considered. The optimal strategy (mission 1) is compared to a simple strategy, which, during mission $1s$

**Table 1   Escape trajectories using Jupiter flyby**

| Mission | Steering | Coast | $E_f$ | $\Delta E_{FB}$ | $P^*$ | $c$ | $I_s$ (s) |
|---------|----------|-------|-------|-----------------|-------|-----|-----------|
| $1s$ | $\boldsymbol{T}\|\boldsymbol{V}$ | No | 0.3250 | 0.1647 | 0.02068[a] | 2.105[a] | 6391[a] |
| 1 | Optimal | No | 0.3670 | 0.2190 | 0.02068[a] | 2.105[a] | 6391[a] |
| 2 | Optimal | No | 0.3671 | 0.2191 | 0.02096[b] | 2.130[a] | 6467[a] |
| $2c$ | Optimal | Yes | 0.3943 | 0.2231 | 0.02167[b] | 2.192[c] | 6655[c] |
| 3 | Optimal | No | 0.4738 | 0.3011 | 0.02071[b] | 1.067–15.822[d] | 3240–48039[d] |
| $3c$ | Optimal | Yes | 0.5312 | 0.2900 | 0.02071[b] | 0.960–3.786[d] | 2915–11495[d] |

[a]Assigned.   [b]Optimal.   [c]Optimal, constant.   [d]Optimal, variable.

(*s* for simple), minimizes the thrust misalignment losses by applying the thrust parallel to the spacecraft velocity. The exhaust power and velocity are $P^* = 0.02068$ (corresponding to 0.55 W of exhaust power per kg of spacecraft initial mass) and $c = 2.105$, which are the best values for the nonoptimal strategy. Figure 1 shows the thrust and velocity directions during the missions. The thrust direction control is largely used before the flyby, to approach Jupiter with a relative velocity that improves the energy increment $\Delta E_{FB}$ received from the planet; after the encounter the thrust is maintained parallel to the velocity. The aim of the optimal strategy is evident in Fig. 2; steering capabilities are used to search for the best approach instead of maximizing the energy increment before the intercept; and an earlier flyby provides the additional benefit of longer engine operation with higher spacecraft velocities. The optimal trajectory (Fig. 3) keeps the spacecraft closer to the sun in order to reduce gravitational losses and anticipate the intercept time.

The improvement provided by the optimal $P^*$ (case 2 in Table 1) is limited, as the optimal power level is close to the value of case 1. Better results derive from the introduction of a coast arc, which is
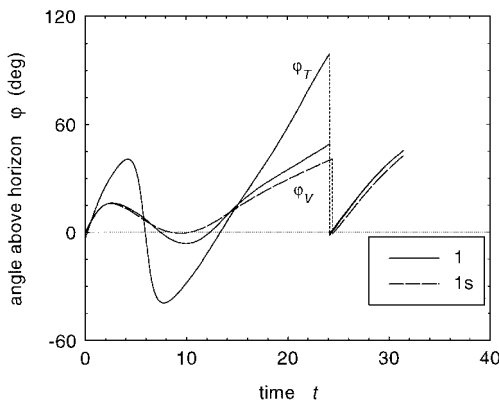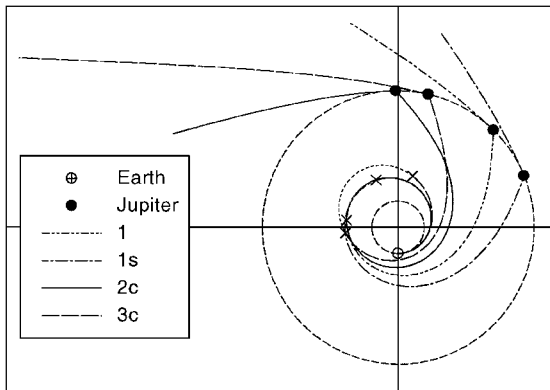
suggested by an examination of the switch function profile during mission 1 (Fig. 4); the improved mission 2c (c for coast) exploits the thrust only when the switching function is positive. The possibility of turning the engine off in the proximity of the first aphelion lowers the following perihelion (see Fig. 3; × marks are used here and in the following figures to identify the extremities of a coast arc) and reduces gravitational losses. Figure 4 also shows that the flyby occurs after a shorter operating time, and a larger amount of propellant can be profitably used after the gravity assist has increased the spacecraft velocity. One should note that the engine is switched off and on at the same distance from the sun ($r = 1.99$).

If the engine is continuously operated with variable exhaust velocity (case 3), low thrust (i.e., high specific impulse) is exploited at the highest radii; high thrust is instead more convenient when the spacecraft is close to the sun in order to reduce gravitational losses. However, it is opportune to switch off the engine (case 3c) in the proximity of the first aphelion passage, where thrust would be extremely low. Some features of this trajectory are highlighted in Fig. 5. The engine is turned off and on again at the same distance from the sun ($r = 2.03$), where c takes the same value.

Table 1 highlights the twofold advantage of an adjustable specific impulse (cases 3 and 3c); the optimal use of the available power increases the energy gain directly, and indirectly, via a better approach to Jupiter and a more efficient flyby. In both cases constraining the periapsis of the planetocentric hyperbola to about 140,000 km, corresponding to a circular velocity $v_p = 1$, has been necessary. During a minimum-height flyby, the steering capabilities of electrical propulsion could be used inside the planet's sphere of influence to increase the turn angle provided by gravitation.

The estimated operative life of a present-technology electric thruster is lower than five years; two years are assumed in the second example, together with a larger value of the power source specific mass ($\beta = 25$, corresponding to 141 kg/kW). The attainable energy increment is not sufficient to reach Jupiter's orbit directly (Fig. 6). The escape energy can instead be obtained by performing a Venus flyby (Fig. 7). Other characteristics of the optimal mission are presented in Figs. 6, 8, and 9. The engine is first used to increase energy



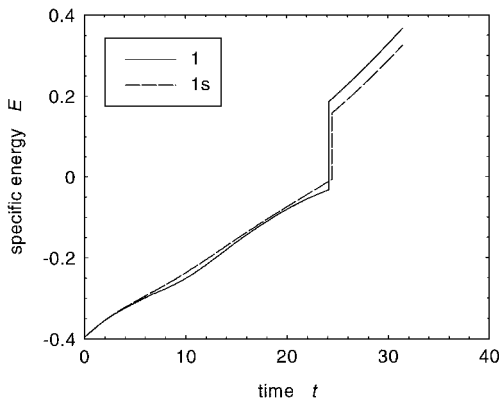Fig. 1 Thrust $\varphi_T$ and velocity $\varphi_V$ directions during missions 1 and 1s.



Fig. 2 Energy increment during missions 1 and 1s.



Fig. 3 Comparison of escape trajectories using Jupiter flyby (see Table 1).
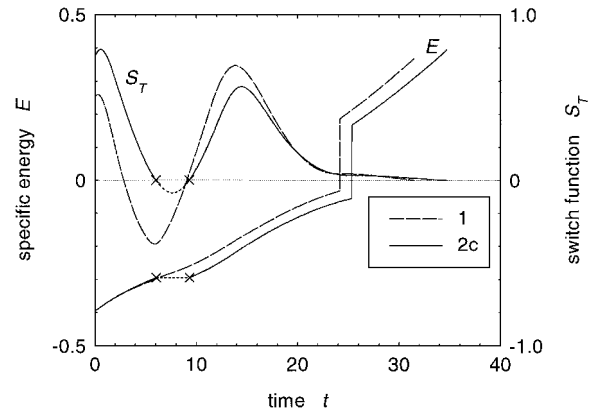


Fig. 4 Benefit of the additional coast arc during mission 2c.
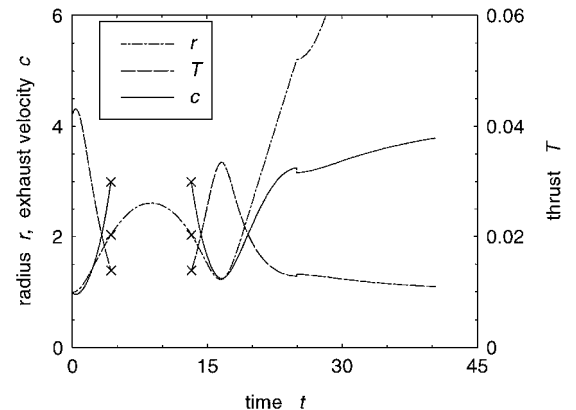


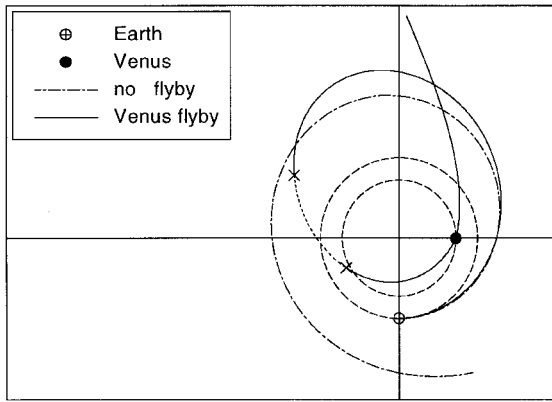Fig. 5 Optimal exhaust-velocity control during mission 3c.
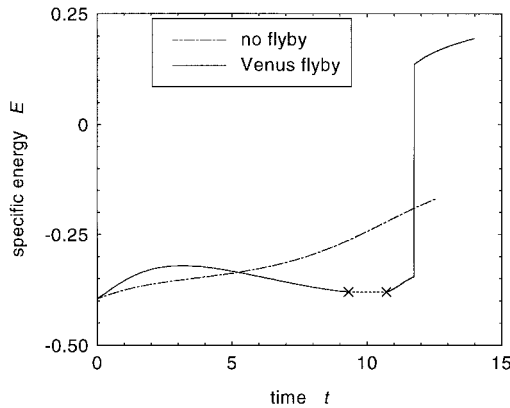
Fig. 6    Escape trajectory using Venus flyby.



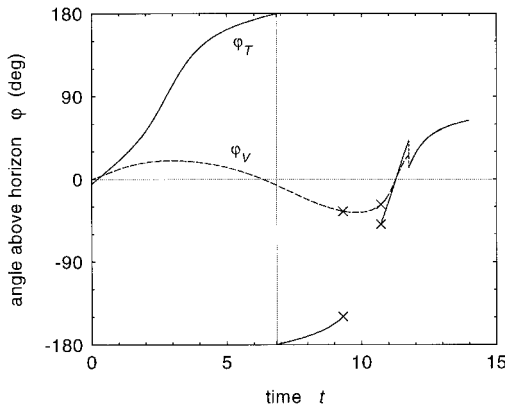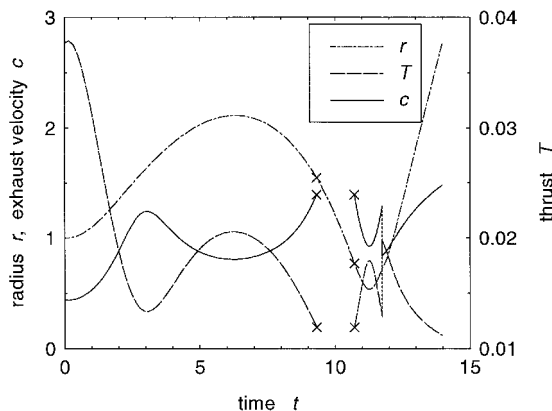Fig. 7    Energy increment provided by Venus flyby.



Fig. 8    Velocity direction $\varphi_V$ and optimal thrust direction $\varphi_T$ for escape using Venus flyby.



Fig. 9    Optimal exhaust-velocity control for escape using Venus flyby.

and aphelion but is also necessary to lower the perihelion in order to intercept Venus' orbit; the thrust direction is gradually misaligned to rotate the velocity vector and eventually to decrease the spacecraft energy. A coast arc is present at intermediate radii, as it is not convenient to rotate a high velocity vector; the engine is again turned on at low radii, when thrust can efficiently be used to increase the spacecraft energy. The exhaust velocity assumes the same value when the engine is turned off and on, but, in this case, the distance from the sun is not the same. A minimum-height flyby is performed with $v_p = 0.25$, corresponding to about a 6400-km periapsis.

## Conclusions

The trajectory of a spacecraft that uses electric propulsion and gravity assist for a deep-space mission has been analyzed. The necessary conditions for optimality have been presented; in particular, the analysis has shown that a power-limited propulsion system requires a bang-bang control if the time constraint concerns the operative life of the thruster instead of the mission time length.

The optimal power level that maximizes the spacecraft specific energy for an assigned payload ratio and engine operating time is easily found using this procedure. It is expressed by a simple algebraic relation between the payload and the power source mass in the case of a thruster that can be continuously throttled.

Numerical examples involving Jupiter or Venus flybys have been presented and used to quantify the benefit of increasing the number of control variables, that is, by augmenting the thrust vector control with the capabilities of adjusting the exhaust velocity and temporarily switching off the thruster.

## Appendix: Coast Arcs

The usefulness of coast arcs when the engine operates with variable specific impulse is shown in this Appendix. The constraint on the engine operating time is written as

$$\int_0^{t_f} \delta(P)\,\mathrm{d}t = \tau \qquad (A1)$$

where the function $\delta(P)$ is null when the engine is turned off ($P = T = 0$) and otherwise unity. This kind of constraint is treated[12] by introducing the constant multiplier $\lambda'$ and adding $\lambda'\delta$ to Eq. (22). The Hamiltonian function becomes

$$H' = H + \lambda'\delta = \boldsymbol{\lambda}_r^T \boldsymbol{v} + \boldsymbol{\lambda}_v^T \boldsymbol{g} + P S_P + \lambda'\delta(P) \qquad (A2)$$

The application of Pontryagin's Maximum Principle states that a bang-bang control is optimal; the control must be set to zero even though $S_P$ is positive, but $P^* S_P + \lambda'$ is negative; and the maximum value $P^*$ is otherwise optimal. As no constraint is explicitly imposed on the final time in this Appendix, $H'_f = 0$, and one easily obtains $\lambda' = -P^* S_{Pf}$. Maximum power is therefore used when $S_P - S_{Pf}$ is positive; unpowered arcs are required in the opposite case.

This control law is peculiar because of the constraint on the engine operating time. A different and well-known result[1,2] is obtained also by means of this analysis if the overall time length of the mission is instead constrained. The function $\delta$ is always unity and does not intervene in the optimization. The power level depends only on the sign of $S_P$, and maximum power is always required when the engine can be operated with a variable specific impulse as $\lambda_m$ and $S_P$ are positive during the whole mission.

## References

[1]Prussing, J. E., "Equation for Optimal Power-Limited Spacecraft Trajectories," *Journal of Guidance, Control, and Dynamics*, Vol. 16, No. 2, 1993, pp. 391–393.

[2]Kechichian, J. A., "Optimal Low-Thrust Transfer Using Variable Bounded Thrust," *Acta Astronautica*, Vol. 36, No. 7, 1995, pp. 357–365.

[3]Pastrone, D., "Traiettorie Ottimali con Flyby," *Atti del XIII Congresso Nazionale*, Associazione Italiana di Aeronautica e Astronautica, Rome, 1995, pp. 1115–1124.

[4]Kluever, C. A., "Heliospheric Boundary Exploration Using Ion Propulsion Spacecraft," *Journal of Spacecraft and Rockets*, Vol. 34, No. 3, 1997, pp. 365–371.

[5]Casalino, L., Colasurdo, G., and Pastrone, D., "Optimization Procedure for Preliminary Design of Opposition-Class Mars Missions," *Journal of Guidance, Control, and Dynamics*, Vol. 21, No. 1, 1998, pp. 134–140.

[6]Kluever, C. A., and Abu-Saymeh, M., "Mercury Mission Design Using Solar Electric Propulsion Spacecraft," *Journal of Spacecraft and Rockets*, Vol. 35, No. 3, 1998, pp. 411–413.

[7]Casalino, L., Colasurdo, G., and Pastrone, D., "Optimization of $\Delta V$-Earth-Gravity-Assist Trajectories," *Journal of Guidance, Control, and Dynamics*, Vol. 21, No. 6, 1998, pp. 991–995.

[8]Bryson, A. E., and Ho, Y. C., *Applied Optimal Control*, Hemisphere, Washington, DC, 1975, pp. 106–108.

[9]Colasurdo, G., Pastrone, D., and Casalino, L., "Optimization of Rocket Ascent Trajectories Using an Indirect Procedure," AIAA Paper 95-3323, Aug. 1995.

[10]Lawden, D. F., *Optimal Trajectories for Space Navigation*, Butterworths, London, 1963, pp. 54–68.

[11]Colasurdo, G., and Pastrone, D., "Indirect Optimization Method for Impulsive Transfers," AIAA Paper 94-3762, Aug. 1994.

[12]Bryson, A. E., and Ho, Y. C., *Applied Optimal Control*, Hemisphere, Washington, DC, 1975, pp. 90, 91.